

Analyst

Accepted Manuscript



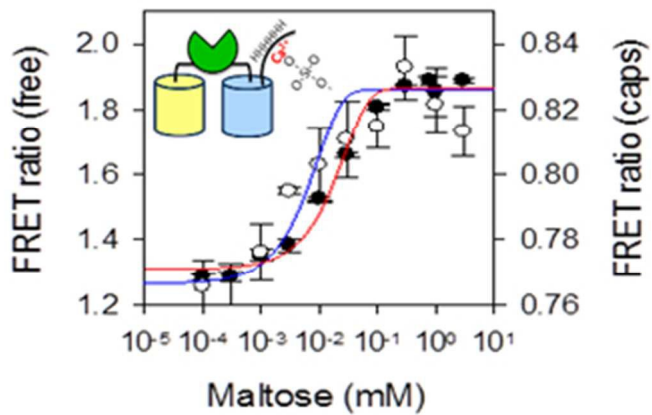
This is an *Accepted Manuscript*, which has been through the Royal Society of Chemistry peer review process and has been accepted for publication.

Accepted Manuscripts are published online shortly after acceptance, before technical editing, formatting and proof reading. Using this free service, authors can make their results available to the community, in citable form, before we publish the edited article. We will replace this *Accepted Manuscript* with the edited and formatted *Advance Article* as soon as it is available.

You can find more information about *Accepted Manuscripts* in the [Information for Authors](#).

Please note that technical editing may introduce minor changes to the text and/or graphics, which may alter content. The journal's standard [Terms & Conditions](#) and the [Ethical guidelines](#) still apply. In no event shall the Royal Society of Chemistry be held responsible for any errors or omissions in this *Accepted Manuscript* or any consequences arising from the use of any information it contains.

1
2
3
4
5
6
7
8
9
10
11
12
13
14
15
16
17
18
19
20
21
22
23
24
25
26
27
28
29
30
31
32
33
34
35
36
37
38
39
40
41
42
43
44
45
46
47
48
49
50
51
52
53
54
55
56
57
58
59
60





ChemComm

COMMUNICATION

Encapsulation of FRET-based glucose and maltose biosensors to develop functionalized silica nanoparticles

Received 00th January 20xx,
Accepted 00th January 20xx

G. Faccio^{†a*}, M. B. Bannwarth^{†b}, C. Schulenburg^a, V. Steffen^c, D. Jankowska^a, M. Pohl^c, R.M. Rossi^b,
K. Maniura-Weber^a, L. F. Boesel^b, M. Richter^{a*}

DOI: 10.1039/x0xx00000x

www.rsc.org/

Silicate nanoparticles with immobilized FRET-based biosensors were developed for the detection of glucose and maltose. Immobilization of the protein biosensor in the nanoparticle was achieved through specific interaction between the hexa-histidine tag of the protein and a calcium-silicate complex of the silica matrix. Encapsulation of the biosensors preserved the affinity for the respective sugar. Compared to the free biosensors, encapsulation had a stabilizing effect on the biosensor towards chemical and thermal denaturation. The demonstrated immobilization strategy for specific sensing proteins paves the way towards the development of protein-inorganic nanostructures for application in metabolite analyses.

Nanoparticles responsive to changes in environmental conditions allow controlled release of entrapped molecules¹, intracellular and targeted delivery², and intracellular sensing³. Based often on polymers, metals⁴, or semiconductors⁵, nanoparticles made of silica have also been used for such purposes. Silica particles are characterized by a low cyto- and genotoxicity, and versions functionalized with inorganic dyes have been described to label and identify cells⁶, and to sense pH^{7, 8}, oxygen⁹, copper ions¹⁰, zinc ions¹¹, and TNT¹². To our knowledge, we report fluorescent silica-protein nanoparticles incorporating FRET-based protein biosensors for the first time and characterize their performance. FRET-based protein biosensors are established for the detection of intracellular

metabolites¹³. This study focuses on two FRET-based biosensors for the detection of glucose and maltose¹⁴⁻¹⁶. These biosensors consist of two fluorescent proteins (enhanced cyan fluorescent protein, ECFP, and enhanced yellow fluorescent proteins EYFP and citrine, respectively) representing a FRET pair and flanking the respective central periplasmic sugar binding protein, like a venus-flytrap.

In this study we encapsulate FRET-based glucose and maltose biosensors in silicate nanoparticles to evaluate whether their immobilization can widen their field of application, e.g. for extracellular metabolite analysis. Besides the protection against the environment, the immobilization of biomolecular biosensors within a matrix allows facile recovery, reuse in successive processes, and often confers improved robustness towards environmental conditions¹⁷. Key challenge during the immobilization of the biosensor is the preservation of the functionality^{18, 19}. Loss of functionality can be due to the harsh conditions often required for immobilization and by direct interaction of the biomolecules with the matrix that can negatively affect the fluorescent signal. The latter is specifically important in the present case as the function of the FRET-based glucose and maltose biosensors relies on the conformational change of the sugar-binding protein upon binding the sugar ligand, resulting in the alteration of the distance and/or orientation of the flanking fluorescent proteins, and thus in a FRET change. The major challenge addressed in this study is the immobilization of the biosensor to a protective matrix thereby preserving the mobility, which is directly correlated with its functionality. Hence, a permanent, yet orthogonal immobilization is required. Therefore, we made use of a specific interaction between an N-terminal hexahistidine tag fused to the ECFP-part of the biosensor with the silica matrix mediated by calcium cations²⁰. This specific interaction was achieved during the heterophase encapsulation procedure in which the hexahistidine-tagged biosensor is located inside of aqueous droplets together with calcium ions, which can coordinate to the silica matrix once silica formation is induced. Therefore, the pH is increased, which leads to the hydrolysis of the precursor tetraethyl

^a Empa, Swiss Federal Laboratories for Materials Science and Technology, Biointerfaces, Lerchenfeldstrasse 5, 9014 St. Gallen (CH)

^b Empa, Swiss Federal Laboratories for Materials Science and Technology, Laboratory for Protection and Physiology Lerchenfeldstrasse 5, 9014 St. Gallen (CH).

^c IBG-1: Biotechnology, Forschungszentrum Jülich GmbH, 52425 Jülich (DE).

*Corresponding author: Dr. Greta Faccio Empa, Swiss Federal Laboratories for Materials Science and Technology, Biointerfaces, Lerchenfeldstrasse 5, 9014 St. Gallen (CH) Tel: +41 58 765 7262 Email: greta.faccio@empa.ch

*Corresponding author: Dr. Michael Richter Current address: Fraunhofer Institute for Interfacial Engineering and Biotechnology IGB, Bio-, Electro and Chemocatalysis BioCat, Straubing Branch, Schulgasse 11a, 94315 Straubing (DE) Tel: +49 9421 187-353 Email: michael.richter@iqb.fraunhofer.de

[†] These authors contributed equally (G.F., M.B.B.).

Electronic Supplementary Information (ESI) available. See DOI: 10.1039/x0xx00000x

COMMUNICATION

orthosilicate (TEOS) and subsequent formation of the silica nanohost (Fig. 1)²⁰. This mild approach favours both the site-specific interaction between the protein and the silica nanohost through the hexahistidine tag, and reduces the adsorption of the negatively charged protein e.g. GFP (pI ~6.2)¹⁴ and the glucose biosensor (calculated pI = 5.6), to the material, e.g. the negatively charged silica.

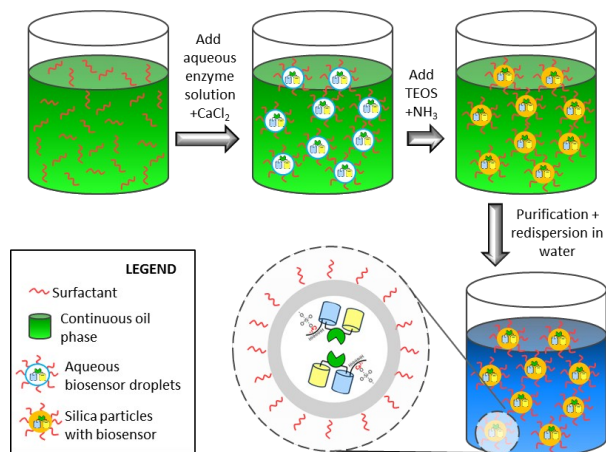


Fig. 1 Schematic illustration of the process for protein encapsulation in silica nanoparticles. After formation of a microemulsion, silica nanoparticles are formed by addition of ammonium hydroxide to increase the pH. In a last step, the inverse microemulsion is redispersed in water to give an aqueous silica dispersion with the FRET-based biosensor encapsulated in the silica nanomatrix. A specific interaction between the silica matrix and the biosensor is mediated by a silica-calcium-hexahistidine-tag complex.

Colloidal analysis of the prepared silica nanohosts containing the sugar biosensors was performed by scanning transmission electron microscopy (STEM) to determine their size and morphology (Fig. 2). The STEM images show spherical nanoparticles with average diameters ~80 nm and similar sizes for the silica particles with encapsulated maltose (Fig. 2A) or glucose biosensor (Fig. 2B). Hence, the type of encapsulated biosensor did not largely influence the size and morphology of the silica particles. The observed sizes are in good agreement with the macroscopic appearance of the dispersion, which shows only little visual turbidity for such small nanoparticles, allowing an analysis of the optical properties of the encapsulated biosensor proteins without large scattering disturbances.

The surface properties of the nanoparticles were investigated *via* zeta potential measurements. The silica particles with encapsulated maltose biosensor yielded a potential of -31.3 ± 3.6 mV and for the encapsulated glucose biosensor -31.9 ± 4.6 mV. Thus, the type of encapsulated biosensor does not influence the surface potential of the silica particles. The obtained zeta potentials of ~-30 mV indicate a moderately stable dispersion not prone to aggregation.

In order to remove free biosensor protein not encapsulated in the silica matrix, the silica nanoparticles were washed several times by centrifugation and redispersion. The presence and integrity of the immobilized biosensors in the silica matrix was then proven by fluorescence microscopy.

Therefore, the purified nanoparticles were diluted in 20 mM MOPS (pH 7.4) and images were taken with a fluorescence microscope (Fig. 2) using a YFP fluorescence filter as described in the Electronic Supplementary Information. A biosensor-specific YFP fluorescence was detected concentrated in small dots not detectable with visible light. However, a small fraction of aggregated nanoparticles could be found (Fig. 2C and D).

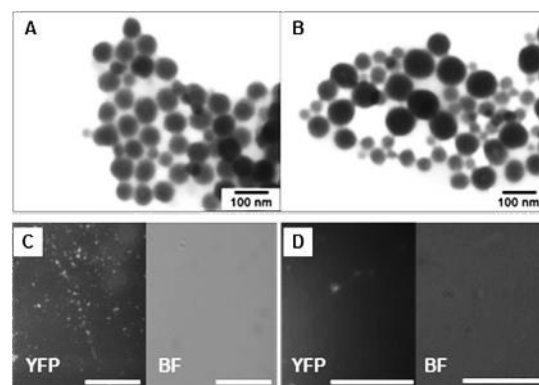


Fig. 2 STEM (A, B) and fluorescence microscopy (C, D) images (BF, bright field, YFP fluorescence filter $\lambda_{ex}=500$ nm and $\lambda_{em}>515$ nm) of silica nanoparticles with encapsulated maltose (left) and glucose (right) biosensors in 20 mM MOPS (pH 7.4). A fraction of aggregated nanoparticles are visible (YFP illumination).

To determine the effect of the immobilization on the fluorescent properties of the biosensor, fluorescence spectroscopy was performed. After immobilization, the fluorescent properties of both fluorescent proteins are preserved. However, the FRET ratio is lower for the encapsulated forms as compared to the free untreated equivalents for both the maltose and glucose biosensor system. The FRET ratio changes from 1.99 to 1.09 for the encapsulated glucose biosensor and from 1.2 to 0.9 for the encapsulated maltose biosensor. This effect can be explained by fluorescence quenching effects inside the nanoparticle. A similar effect has also been observed when the FRET ratios of such biosensors were measured inside *E. coli* cells (V. Steffen, unpublished). The sensing capabilities of the functionalized nanoparticles were investigated by recording binding isotherms for maltose and glucose, respectively, over a wide range of sugar concentrations covering four orders of magnitude (Fig. 3A and 3B). The samples were pre-incubated in the presence of different sugar concentrations for two hours to ensure equilibrium conditions. The fluorescence spectrum of the individual solutions were measured and the FRET ratio was calculated as the ratio between the fluorescence intensity emitted at 528 nm and at 485 nm ($\lambda_{ex}=428$ nm). The affinity (K_d) of the entrapped biosensors was calculated and resulted in the same order of magnitude as determined for the biosensors in free form, e.g. 1.6 vs. 6.4 mM glucose and 0.2 vs. 0.1 mM maltose for the glucose and maltose biosensors in the free and encapsulated forms, respectively. These results demonstrate that the porosity of the nanocapsules is high enough to allow permeation of low-molecular weight metabolites while simultaneously entrapping the proteins.

In order to assess the effect of encapsulation towards chemical denaturation, both the free sugar biosensor proteins and their encapsulated versions were incubated in the presence of different concentrations of urea. The effect of encapsulation on the biosensor was determined *via* the change in FRET ratio as a function of the urea concentration. As shown in Fig. 3, encapsulation had a stabilizing effect toward urea. Above 3 M urea, the functionalized nanoparticles containing the maltose biosensor maintained a higher FRET ratio compared to the equivalent free protein (Fig 3C). Major changes in FRET ratio were detected in the presence of 0-2 M urea for the glucose biosensor for both the free and encapsulated form, with the encapsulated form being more stable (Fig 3D).

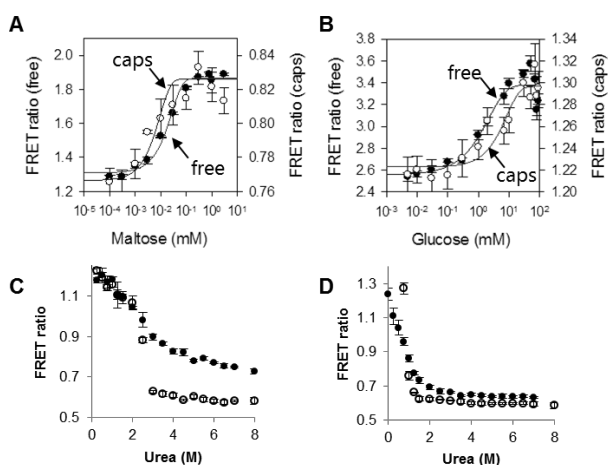


Fig. 3 Changes in FRET ratio of the maltose (A and C) and glucose (B and D) biosensor when in the presence of 0.0005-100 mM maltose (A) or 0.005-100 mM glucose (B), respectively, or 0-8 M urea (C and D). The encapsulated biosensors (empty dots) and free biosensors (filled dots) are reported and fitted with a Sigmoidal Dose Response tool of SigmaPlot (Systat Software Inc.). More detailed results in Fig. S1 and S2. Data reported as average \pm SEM, $n > 3$.

Similarly, the functionalized nanoparticles with the maltose biosensor retained a slightly higher FRET ratio upon thermal treatment by incubation at 70°C (Fig. S3, S4). The functionalized nanoparticles with the glucose biosensor showed the same behaviour as the free biosensor at different pH conditions with increasing FRET ratios at increasing pH and reaching a maximum at pH = 7.5-8 (Fig. S5, S6).

In conclusion, silica nanoparticles responsive to glucose or maltose were assembled by incorporating two specific FRET-based protein biosensors. The functionalized nanoparticles had affinity for glucose or maltose similar to the free biosensor protein and showed an enhanced performance towards denaturation by urea and temperature. Moreover, they were highly permeable to small molecules. Functional nanoparticles converting the local concentration of a metabolite, e.g. glucose or maltose, into a fluorescent signal could be prepared by combining an inorganic support such as silica with the specificity provided by FRET-based protein biosensors. Our

concept developed here is very promising not only for *in vitro* sensing metabolites, e.g. in biological fluids, but also for *in vivo* metabolite analysis.

This research was supported by a grant from the Swiss Confederation and funded by Nano-Tera.ch within the Nano-Tera project "Fabrication of fluorescence biosensors in a Textile Dressing for Non-invasive Lifetime Imaging-based Wound Monitoring", FLUSITEX (RTD 2013) that was scientifically evaluated by the SNSF.

Notes and references

- M. B. Bannwarth, S. Ebert, M. Lauck, U. Ziener, S. Tomcin, G. Jakob, K. Münnemann, V. Mailänder, A. Musyanovych and K. Landfester, *Macromolecular Bioscience*, 2014, **14**, 1205-1214.
- I. I. Slowing, B. G. Trewyn and V. S. Lin, *J. Am. Chem. Soc.*, 2007, **129**, 8845-8849.
- M. Motornov, Y. Roiter, I. Tokarev and S. Minko, *Progress in Polymer Science*, 2010, **35**, 174-211.
- K. Saha, S. S. Agasti, C. Kim, X. Li and V. M. Rotello, *Chem. Rev.*, 2012, **112**, 2739-2779.
- L. Shang and G. U. Nienhaus, *Materials Today*, 2013, **16**, 58-66.
- H. Liu, S. Wu, C. Lu, M. Yao, J. Hsiao, Y. Hung, Y. Lin, C. Mou, C. Yang, D. Huang and Y. Chen, *Small*, 2008, **4**, 619-626.
- T. Ye, Y. Du, C. He, B. Qiu, Y. Wang and X. Chen, *Anal. Methods*, 2012, **4**, 1001-1004.
- S. Widmer, M. J. Reber, P. Müller, C. E. Housecroft, E. C. Constable, R. M. Rossi, D. Bruhwiler, L. J. Scherer and L. F. Boesel, *Analyst*, 2015, **140**, 5324-5334.
- M. J. Ruedas-Rama, J. D. Walters, A. Orte and E. A. H. Hall, *Anal. Chim. Acta*, 2012, **751**, 1-23.
- C. Zong, K. Ai, G. Zhang, H. Li and L. Lu, *Anal. Chem.*, 2011, **83**, 3126-3132.
- P. Teolato, E. Rampazzo, M. Arduini, F. Mancin, P. Tecilla and U. Tonellato, *Chemistry – A European Journal*, 2007, **13**, 2238-2245.
- D. Gao, Z. Wang, B. Liu, L. Ni, M. Wu and Z. Zhang, *Anal. Chem.*, 2008, **80**, 8545-8553.
- W. B. Frommer, M. W. Davidson and R. E. Campbell, *Chem. Soc. Rev.*, 2009, **38**, 2833-2841.
- R. Moussa, A. Baierl, V. Steffen, T. Kubitzki, W. Wiechert and M. Pohl, *J. Biotechnol.*, 2014, **191**, 250-259.
- K. Deuschle, S. Okumoto, M. Fehr, L. L. Looger, L. Kozhukh and W. B. Frommer, *Protein Science*, 2005, **14**, 2304-2314.
- M. Fehr, W. B. Frommer and S. Lalonde, *Proceedings of the National Academy of Sciences*, 2002, **99**, 9846-9851.
- C. Mateo, J. M. Palomo, G. Fernandez-Lorente, J. M. Guisan and R. Fernandez-Lafuente, *Enzyme Microb. Technol.*, 2007, **40**, 1451-1463.
- A. Sassolas, L. J. Blum and B. Leca-Bouvier, *Biotechnol. Adv.*, 2012, **30**, 489-511.
- G. Faccio, M. M. Kämpf, C. Piatti, L. Thöny-Meyer and M. Richter, *Sci. Rep.*, 2014, **4**.
- A. Cao, Z. Ye, Z. Cai, E. Dong, X. Yang, G. Liu, X. Deng, Y. Wang, S. Yang, H. Wang, M. Wu and Y. Liu, *Angewandte Chemie International Edition*, 2010, **49**, 3022-3025.

1
2
3
4 **ChemComm**
5
67
8 **COMMUNICATION**
910
11 **Supplementary information**
1213
14
15 **Encapsulation of FRET-based glucose and maltose biosensors to develop**
16 **functionalized silica nanoparticles**
1718
19 G. Faccio^{†*}, M. B. Bannwarth^{†b}, C. Schulenburg^a, V. Steffen^c, D. Jankowska^a, M. Pohl^c, R.M. Rossi^b, K. Maniura-Weber^a, L. F. Boesel^b, M.
20 Richter^{a*}
2122
23
24
25
26
27
28 ^a Biointerfaces, Empa - Swiss Federal Laboratories for Materials Science and Technology, Lerchenfeldstrasse 5, 9014 St. Gallen (CH).
2930 ^b Laboratory for Protection and Physiology, Empa - Swiss Federal Laboratories for Materials Science and Technology, Lerchenfeldstrasse 5,
31 9014 St. Gallen (CH).
3233 ^c IGB-1: Biotechnology, Forschungszentrum Jülich GmbH, 52425 Jülich (DE).
3435
36
37
38 *Corresponding author: Dr. Greta Faccio39 Laboratory for Biointerfaces, Empa - Swiss Federal Laboratories for Materials Science and Technology, Lerchenfeldstrasse 5, 9014 St. Gallen
40 (CH) Tel: +41 58 765 726241 Email: greta.faccio@empa.ch
42

43 *Corresponding author: Dr. Michael Richter

44 Current address: Fraunhofer Institute for Interfacial Engineering and Biotechnology IGB, Bio-, Electro and Chemocatalysis BioCat, Straubing
45 Branch, Schulgasse 11a, 94315 Straubing (D) Tel: +49 9421 187-35346 Email: michael.richter@igb.fraunhofer.de
47
48
49
50
51
52
53
54
55
56
57
58
59
60

Journal Name

COMMUNICATION

Experimental**Chemicals and proteins**

Chemicals for the biochemical characterization of the sugar biosensors were purchased from Sigma Aldrich (Buchs, Switzerland). In particular, D-(+)-Maltose monohydrate BioUltra, $\geq 99.0\%$ (HPLC) (product nr. 63418) and D-(+)-Glucose monohydrate for microbiology, $\geq 99.0\%$ (Fluka) (product nr. 49159) were purchased from Sigma Aldrich (Buchs, CH) and used as analytes. All commercially available chemical reagents and solvents were used without further purification. Triton X-100 and tetraethyl orthosilicate (TEOS) were purchased from Sigma Aldrich (Buchs, Switzerland). Proteins were expressed and purified as described elsewhere¹ and stored in 20 mM MOPS, pH 7.4 at -20°C .

FRET-based sugar biosensors

The glucose biosensor pRSET FLII¹²Pglu600 μ ^{2, 3} and the maltose biosensor pRSET FLIPmal-25 μ ⁴ were from Addgene (<http://www.addgene.org>). Their expression, purification, and sequences are described in¹.

Formation of silica-sensor nanoparticles

The encapsulation procedure of the protein biosensors was carried out similarly to the protocol described by Cao et al.⁵ In brief, 2 ml of the respective sugar biosensor solution (1 mg/ml initial concentration) in 20 mM MOPS (pH 7.4) were used for the encapsulation process and 2.0 mg of CaCl_2 as well as 200 μL tetraethyl orthosilicate (TEOS) solution added. Separately, a mixture of 10 ml cyclohexane, 2 ml Triton X-100 and 2 ml *n*-hexanol was prepared and mixed mechanically (1400 rpm). Subsequently, the biosensor protein solution was added and the mixture was continuously stirred for 15 min before 100 μL of aqueous 25% ammonium hydroxide solution were injected to start the silica formation. After stirring over night at room temperature, 30 ml of acetone were added and the mixture centrifuged at 2000 rpm. The particles were redispersed in aqueous solution and again precipitated and centrifuged. The procedure was repeated 2 times and the precipitate finally redispersed in 2 ml of water containing 0.1wt.% of SDS.

Microscopy of the encapsulated biosensors

For light microscopy, the biosensors in the silica nanoparticles were diluted ten-folds in 20 mM MOPS (pH 7.4) and imaged with a Leica DM6000 microscope (Leica, United Kingdom) equipped with a digital camera (Leica Digital camera DFC350 FX, Germany) using a fluorescence microscope under bright light and with a GFP filter for fluorescence ($\lambda_{\text{ex}} = 450\text{-}490\text{nm}$, $\lambda_{\text{em}} = 425\text{-}550\text{nm}$) or YFP ($\lambda_{\text{ex}} = 500\text{-}520\text{nm}$, $\lambda_{\text{em}} = 530\text{-}535\text{nm}$).

Scanning transmission electron microscopy (STEM) was performed on a Hitachi S-4800 (Hitachi High technologies, Canada). For sample preparation, an aqueous dispersion of biosensor protein-encapsulated silica nanoparticles as obtained after synthesis was diluted with deionized water (1:50) and drop-casted on 300 mesh carbon coated copper grids and sputtered with gold (Polaron Equipment, SEM coating Unit E5100, Kontron AG, Switzerland, 5 nm thick coating) before imaging.

Biochemical characterization of the encapsulated biosensors

Fluorescence measurements were performed with a Cary Eclipse Fluorescence Spectrophotometer equipped with a multiwell-plate reader (Varian) in black 96-well half-area plates at room temperature using a 100 μL sample. Typically, 10 μL of encapsulated biosensor or 5 μL of the free biosensor (1 mg/ml) were incubated in 20 mM MOPS (pH 7.4), in the presence of various concentrations of maltose or glucose, or urea for 2 hours. For temperature stability studies, the samples were incubated at 70°C without stirring. Fluorescence spectra were recorded with a $\lambda_{\text{ex}} = 428\text{nm}$ and $\lambda_{\text{em}} = 450\text{-}600\text{nm}$. Changes in the biosensor were calculated as variations in the FRET ratio calculated as the ratio between the maximum fluorescence emitted at 528 nm (YFP, Citrine) and at 485 nm (ECFP, $\lambda_{\text{ex}} = 428\text{nm}$).

To test the performance at different pH conditions the sugar biosensors either in free form or entrapped in nanoparticles (10 μL) were incubated for 1 hr at 250 rpm at room temperature with 20 mM MOPS solution (90 μL) at pH values between 4 and 8. Data analysis was performed with SigmaPlot (Systat Software Inc.).

Zeta-potential measurement of the encapsulated biosensors

For zeta potential measurements an aqueous dispersion of the silica nanoparticles with encapsulated sugar biosensors was diluted (1:100) with a 1 mM KCl solution. The resulting dispersion was measured on a Zetasizer Nano ZS90 (Malvern Instruments).

COMMUNICATION

1
2
3
4
5
6
7
8
9
10
11
12
13
14
15
16
17
18
19
20
21
22
23
24
25
26
27
28
29
30
31
32
33
34
35
36
37
38
39
40
41
42
43
44
45
46
47
48
49
50
51
52
53
54
55
56
57
58
59
60

Analyst Accepted Manuscript

Figures

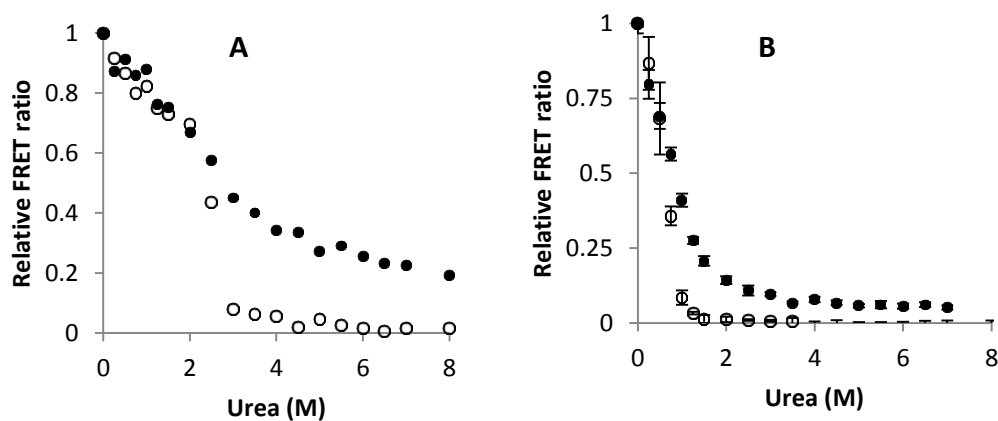


Fig. S1 Relative changes in FRET ratio of the maltose biosensor (A) and glucose (B) biosensor at increasing urea concentrations. Values are reported as average \pm standard deviation.

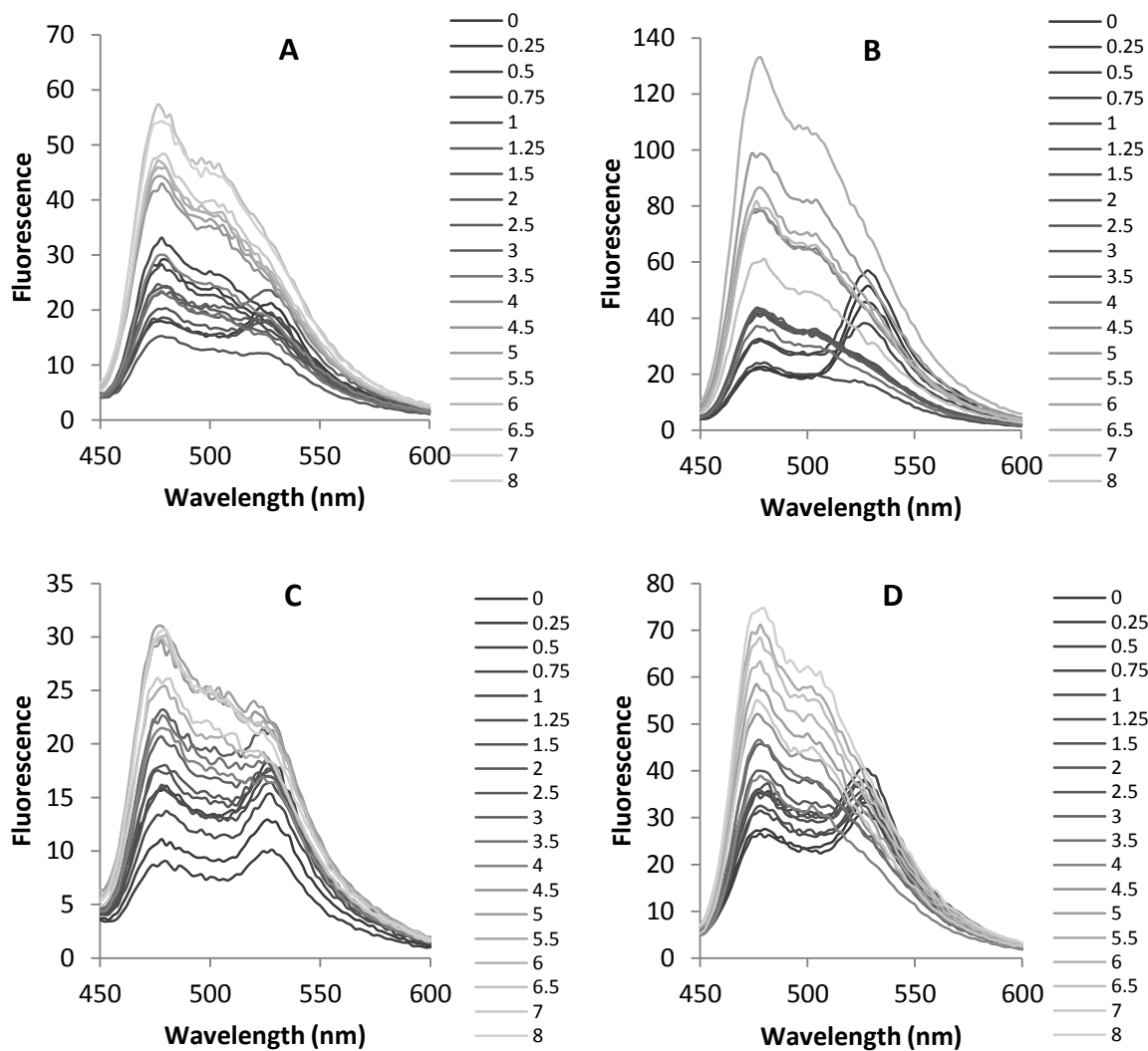


Fig. S2 Fluorescence emission spectra of the glucose (A,B) and maltose (C,D) biosensors in encapsulated (A,C) and free form (B,D) in the presence of urea (reported as molar concentration in the legends). A) Functionalized silica particles containing the glucose biosensor, B) glucose biosensor in free form, C) functionalized silica particles containing the maltose biosensor, D) maltose biosensor in free form.

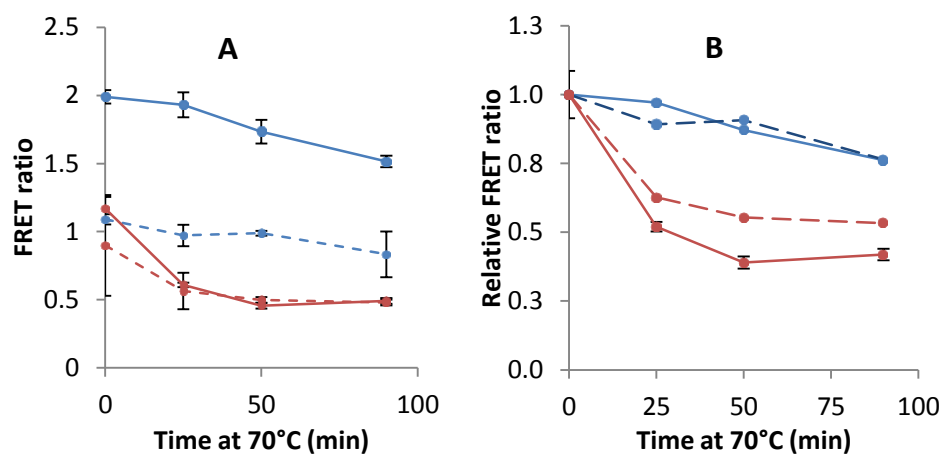


Fig. S3 Absolute (A) and relative (B) FRET ratio changes upon incubation at 70°C for the glucose (blue lines) or maltose (red lines) biosensor as free form (continuous line) or functionalized nanoparticle (dashed line). Values are reported as average \pm standard deviation.

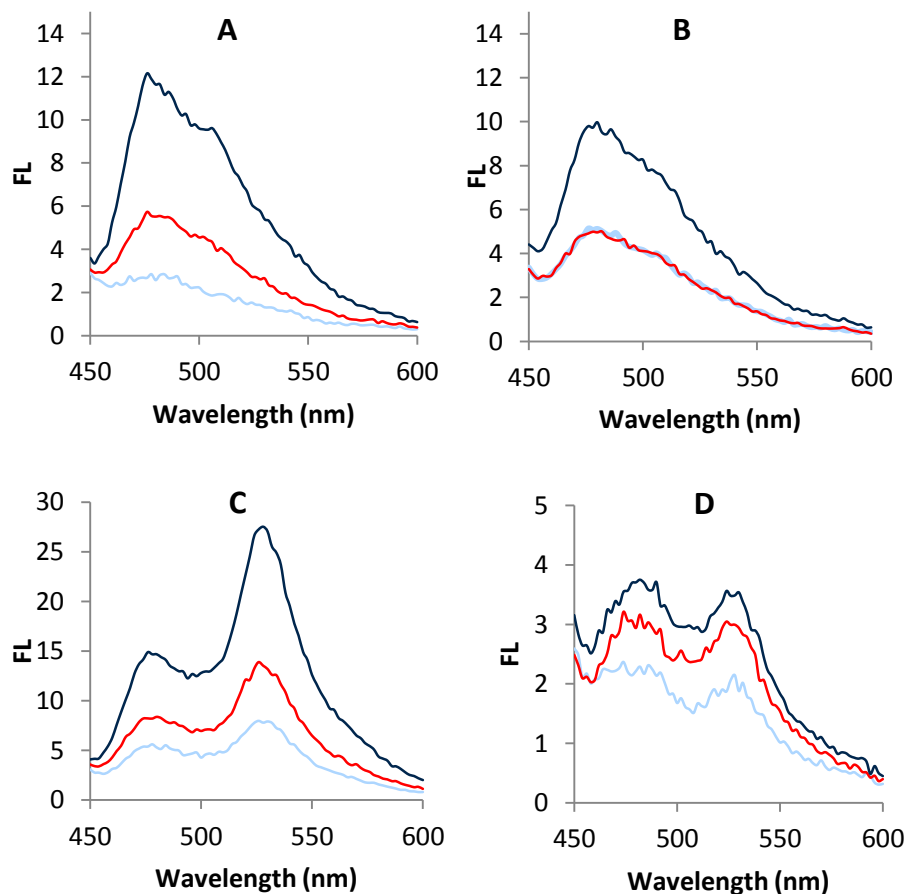


Fig. S4 Fluorescence emission spectra of the glucose and maltose biosensors as functionalized silica nanoparticles or in free form after incubation at 70°C for 25 (dark blue line), 50 (red line), or 90 (light blue line) min. A) Functionalized silica particles containing the glucose biosensor, B) glucose biosensor in free form, C) functionalized silica particles containing the maltose biosensor, D) maltose biosensor in free form.

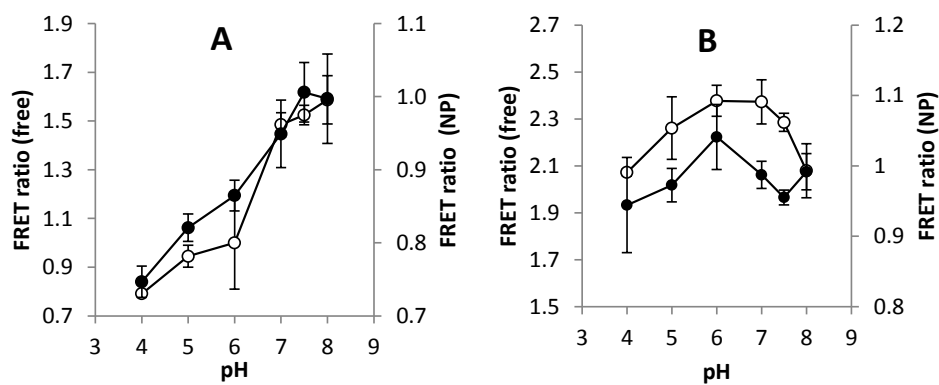


Fig. S5 FRET ratio dependency on the pH of the biosensor environment of the maltose (A) and glucose (B) biosensors in the free (empty dots) and the nanoparticles (filled dots) form. Values are reported as average \pm standard deviation.

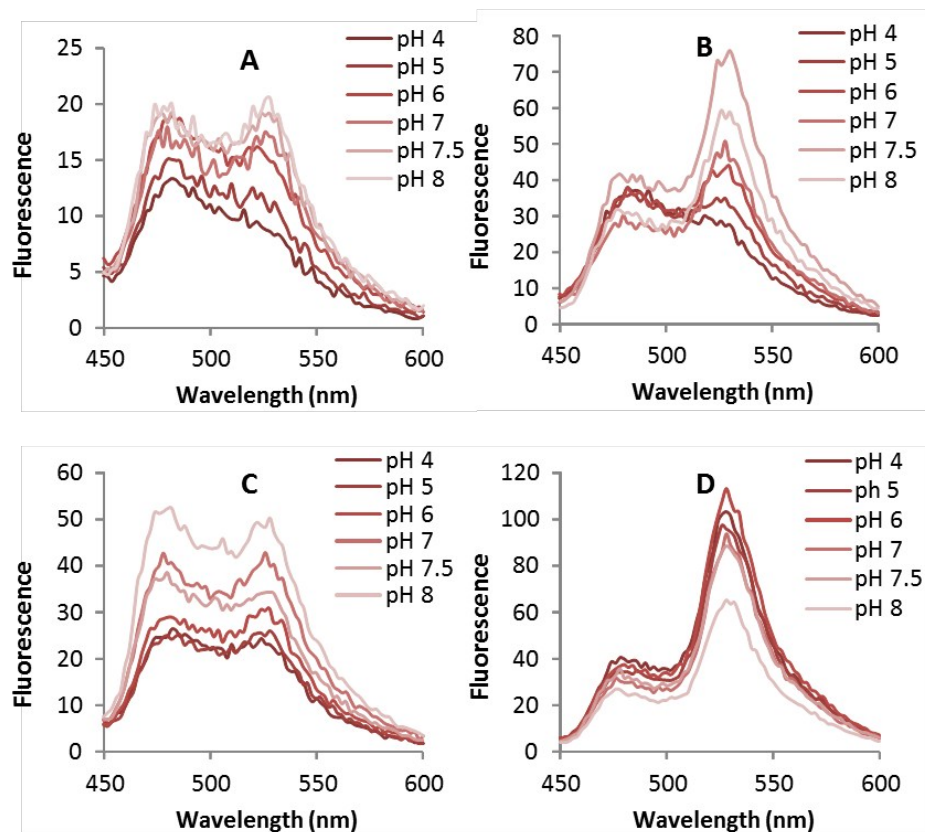


Fig. S6 Fluorescence emission spectra of glucose and maltose biosensors in free or as protein-silica nanoparticles under different pH conditions. A) Functionalized silica particles containing the maltose biosensor, B) maltose biosensor in free form, C) functionalized silica particles containing the glucose biosensor, D) glucose biosensor in free form.

References

- 1 R. Moussa, A. Baierl, V. Steffen, T. Kubitzki, W. Wiechert and M. Pohl, *J. Biotechnol.*, 2014, **191**, 250-259.
- 2 K. Deuschle, S. Okumoto, M. Fehr, L. L. Looger, L. Kozhukh and W. B. Frommer, *Protein Science*, 2005, **14**, 2304-2314.
- 3 M. Fehr, S. Okumoto, K. Deuschle, I. Lager, L. L. Looger, J. Persson, L. Kozhukh, S. Lalonde and W. B. Frommer, *Biochem. Soc. Trans.*, 2005, **33**, 287-290.
- 4 M. Fehr, W. B. Frommer and S. Lalonde, *Proceedings of the National Academy of Sciences*, 2002, **99**, 9846-9851.
- 5 A. Cao, Z. Ye, Z. Cai, E. Dong, X. Yang, G. Liu, X. Deng, Y. Wang, S. Yang, H. Wang, M. Wu and Y. Liu, *Angewandte Chemie International Edition*, 2010, **49**, 3022-3025.